Nanosized carriers for hydrophobic compounds based on mesoporous silica: synthesis and adsorption properties*

A. R. Ibragimova,[a]★ D. R. Gabdrakhmanov,[a] A. R. Khamatgalimov,[a] A. F. Saifina,[a] A. T. Gubaidullin,[a] S. R. Egorova,[b] A. A. Lamberov,[b] M. P. Danilaev,[c] and L. Ya. Zakharova[a]

[a]*Arbuzov Institute of Organic and Physical Chemistry, FRC Kazan Scientific Center, Russian Academy of Sciences, 8 ul. Akad. Arbuzova, 420088 Kazan, Russian Federation. E-mail: alsu_i@iopc.ru*
[b]*Kazan (Volga Region) Federal University, 18 ul. Kremlevskaya, 420008 Kazan, Russian Federation*
[c]*A. N. Tupolev Kazan National Research Technical University — KAI, 10 ul. K. Marksa, 420111 Kazan, Russian Federation*

MCM-41 type mesoporous silica particles were obtained using a template method in an alkaline medium and cetyltrimethylammonium bromide as a matrix. The structural and adsorption characteristics of the mesoporous material were studied by dynamic light scattering, scanning electron microscopy, low-temperature adsorption—desorption of nitrogen, IR spectroscopy, and simultaneous thermal analysis. It was shown that the obtained mesoporous material possesses high porosity with the specific pore volume in excess of 1 $cm^3\ g^{-1}$. It was established that the size of silica particles does not exceed 200 nm, which is a value acceptable for the penetration of drugs through cell membranes. The optimal compositions of aqueous dispersions of MCM-41 with minimal sedimentation processes were determined. A drug (indomethacin) was encapsulated into the silica pores using the precipitation method at various temperatures (40 and 60 °C), the quantitative parameters of loading efficiency were calculated. The influence of temperature on the encapsulation ability was demonstrated.

Key words: template synthesis, MCM-41 type mesoporous silica, indomethacin, adsorption.

Insignificant solubility and low selectivity of drugs are issues of vital importance in modern medicine and pharmacology. About 40% of commercially available drugs or new drugs that pass different stages of trials are practically insoluble in water.[1—6] One of the ways of addressing this problem is through the use of various carriers, which allow the drug to be transferred to a more soluble stable form.[7] Different approaches are currently used, for example, compositions based on lipids[8] or solid dispersions,[9,10] *etc*. One of the most promising approaches is adsorption on a porous carrier (mesoporous material), in particular, on that based on silica (2 nm ≤ pore diameter (D) ≤ 50 nm).[11]

The possibility of using nanoparticles based on mesoporous silicon dioxide as a drug delivery system is being studied. Much attention is being directed toward addressing problems related to systemic toxicity.[12] There are published examples of the successful use of mesoporous silica particles for intravenous drug administration in rats.[13,14] The cytotoxicity of mesoporous silica particles depends on many factors; among them are the number of surface silanol groups, which cause hemolysis,[15] surface charge (cytotoxicity decreases on going from negatively to positively charged particles), as well as the concentration of empty and drug-loaded nanoparticles.[13,16]

The problem of biodegradability of mesoporous silica is also being considered.[17] The possibility of biodegradation of silica nanomaterials over several days was shown. The factors which make it possible to control the rate of biodegradation were established. They include porosity, size, morphology of nanoparticles, the possibility of functionalization of the surface, and alteration of the degradation medium.[18] In a review[18] discussing the problem of removal of drug carriers based on mesoporous silicon, evidence is presented that silica particles are removed from the liver, spleen, heart, kidneys, brain, and lungs within four weeks. The intravenous administration of SiO_2 nanoparticles loaded with an acetylcholinesterase reactivator in rats is described.[14] It was shown that the drug penetrates through the blood-brain barrier, whereby 94% of the particles are removed from the brain within a week and have no effect on the behavior of the rats.

The possibility of varying the size of pores of mesoporous silica materials is shown,[19—23] their large specific

* Dedicated to Academician of the Russian Academy of Sciences A. I. Konovalov on the occasion of his 85th birthday.

Published in Russian in *Izvestiya Akademii Nauk. Seriya Khimicheskaya,* No. 7, pp. 1358—1365, July, 2019.
1066-5285/19/6807-1358

surface area and high volume make it possible to obtain agents with a high content of biologically active substances. At the same time, the presence of voids in silica prevents the aggregation of drug molecules and increases its stability. Surface silanol groups can be used to design active sites of various nature on the silica surface. These sites facilitate the immobilization of drugs, their retention and release at a rate required for efficient therapeutic action.[6,24]

However, there are a number of problems requiring further research. In particular, an increase in the specific surface and volume of pores could considerably increase the efficiency of drug encapsulation. It is also necessary to develop new methods for the encapsulation of drugs into the pores of silica particles. Among the existing methods, the most frequently used are the sequential evaporation of solvents; the melting method, which consists of heating the substance and silica above the melting point of the drug, and the deposition method.[25,26] The main disadvantage of the first two methods is that they do not include the removal of drugs adsorbed on the surface of silica after its loading.[27,28] Despite significant progress in the use of mesoporous silica as a drug carrier, the efficiency of medicinal agent encapsulation is usually low,[5,28—31] excepting certain cases.[5]

The goal of the present work is to synthesize MCM-41 type mesoporous silica, obtain quantitative characteristics of the sample, determine the factors affecting its sorption properties, and investigate the use of the obtained material for drug delivery. Hydrophobic indomethacin was used as a model drug.[32,33]

Experimental

Hexadecyltrimethylammonium bromide (CTAB, ≥99%, Sigma), an aqueous solution of NH_4OH (25 wt.%, TatChem-Product, Russia), tetraethoxysilane (TEOS, ≥99%, Aldrich), indomethacin (99%, Aldrich) were used as reactants for the synthesis of mesoporous silica material. Adsorption and desorption processes were carried out in ethanol (water content no more than 4%). Water passed through the Milli-Q purification system was used as a solvent and dispersion medium in the preparation of samples.

Synthesis of MCM-41 type mesoporous silica. The MCM-41 type mesoporous silica was obtained using a template method described earlier.[34,35] The synthesis was carried out at room temperature (25 °C). A weighed amount of CTAB (2 g) was dissolved in distilled water (270 mL), followed by the addition of an aqueous solution of NH_4OH (205 mL, 25 wt.%). Then, TEOS (10 mL) was added dropwise to the resulting solution with continuous stirring. The reaction mixture was stirred for 10 min and then thermostated at room temperature for 2 h. The white precipitate formed was filtered, washed with several portions of distilled water (5×100 mL), dried in air at room temperature (25 °C) for 6 h. The resulting precipitate was calcined in a muffle furnace at 550 °C for 5 h. The product yield was 45% calculated based on initial TEOS amount.

Encapsulation of indomethacin. Samples of mesoporous silica containing encapsulated indomethacin (MCM-41@IMC-40) were prepared as follows. A weighed amount of indomethacin (100 mg) was dissolved in ethanol (3 mL) at 40 °C, followed by the addition of powdered MCM-41 type mesoporous silica (300 mg) with continuous stirring (550 rpm). The encapsulation procedure was carried out with continuous stirring for 3 h. After that, the mixture was filtered, washed with ethanol (40 °C), and dried at room temperature. The preparation of silica particles containing the encapsulated drug at a temperature of 60 °C (MCM-41@IMC-60) was carried out similarly.

Efficiency of indomethacin encapsulation. The obtained MCM-41@IMC-40 and MCM-41@IMC-60 samples were washed on the filter with five portions of ethanol (3 mL each) and the content of non-encapsulated indomethacin in the collected washings was analyzed by spectrophotometry (a Specord 250 PLUS spectrophotometer (Analytik Jena)), using the known indomethacin extinction coefficient (4382 L mol^{-1} cm^{-1} at λ = 320 nm in ethanol). All measurements were carried out in a 1 cm pathlength cell. The spectra were recorded in the 200—700 nm wavelength range at 25 °C.

The quantitative parameters determining encapsulation efficiency were encapsulation efficiency (E_{enc}) and loading capacity (E_{load}), which were calculated using the following equations:

$$E_{enc} = [(m_0 - m_{unload})/m_0] \cdot 100\%, \quad (1)$$

$$E_{load} = [(m_0 - m_{unload})/m_{SiO_2}] \cdot 100\%, \quad (2)$$

where m_0 is the initial weight of the loaded drug, g; m_{unload} is the weight of the drug which did not bind to silica particles, g; m_{SiO_2} is the weight of mesoporous silica.

Physicochemical characterization of mesoporous material and dispersions based on it. Experiments on dynamic and electrophoretic light scattering were carried out using a Zetasizer Nano nanoparticle analyzer (Malvern). A gas He—Ne laser (4 mW, 633 nm wavelength) was used as a source of laser radiation. All measurements were performed at a constant scattering angle (173°). Particle sizes were determined according to the Stokes—Einstein equation for spherical particles:

$$D = kT/(6\pi\eta R), \quad (3)$$

where k is the Boltzmann constant, T is the absolute temperature, η is the solvent viscosity, R is the hydrodynamic radius. Before measurements, all solutions were filtered through Millipore filters with a pore diameter of 450 nm to remove dust.

X-ray analysis was performed on a D8 Advance X-ray diffractometer (Bruker) equipped with a Vario attachment and a Vantec linear coordinate detector. Cu-Kα_1 radiation (λ = 1.54063 Å) monochromatized with a Johansson curved crystal was used at 40 kV and 40 mA. The powdered samples were smeared on the single-crystal silicon plate. The samples were scanned over the $1 \le 2\theta° \le 50$ range with a step of 0.008° and an acquisition time of 0.1—1 s per point. The data were processed using the EVA software package.

Porous characteristics of the mesoporous silica sample were determined by low-temperature adsorption—desorption of nitrogen using a Quantachrome Autosorb-iQ multi-purpose analyzer (Quantachrome Instruments, USA). Adsorption isotherms were obtained at −196 °C after degassing the sample at 500 °C to a residual pressure of 0.013 Pa. The specific surface was determined using a BET model, the nitrogen molecular area was assumed to be 0.162 nm^2, the density of N_2 in the normal

liquid state, 0.808 g cm^{-3}. The measurement accuracy was 0.1 m^2 g^{-1}±5%. The total pore volume and the mesopore size distribution was calculated from the desorption curve using the Barrett—Joyner—Halenda (BJH) model.[36] The measurement accuracy was ±5%.

The size and morphology of the porous carrier was determined by scanning electron microscopy using an EVO 50XVP electron microscope in combination with an INCA-350 energy dispersive spectrometer (Carl Zeiss). The spectrometer resolution was 130 eV. The analysis was carried out at an accelerating voltage of 20 kV and a distance of 8 mm from the flange.

The content of substances in the MCM-41 mesoporous silica material was evaluated based on IR spectra, which were recorded on a Vector 22 Fourier-transform IR spectrometer (Bruker). Samples were finely ground using KBr granules, the spectra were recorded in the 4000—400 cm^{-1} frequency range with a spectral resolution of 4 cm^{-1}.

Indomethacin encapsulated in mesoporous silica was studied by simultaneous thermal analysis (thermogravimetry (TG)/differential scanning calorimetry (DSC) in combination with infrared Fourier spectroscopy), in which the change in the sample weight is recorded as a function of temperature and the corresponding thermal effects are monitored. A coupled system of a STA449-F3 TG/DSC simultaneous thermal analysis instrument (Netzsch) and a Tensor 27 Fourier-transform IR spectrometer (Bruker)) was used in this work. The samples under study (10.8—13.4 mg) were heated in a corundum crucible (Al_2O_3) with a perforated lid from room temperature to 1000 °C with an empty crucible as a reference sample. The TG/DSC measurements were carried out at a heating rate of 10 °C min^{-1} in a stream of argon of 50 mL min^{-1}. The gas cell and the transport line between the TG/DSC and the IR Fourier-transform spectrometer were heated to 200 and 195 °C, respectively. The infrared spectra of finely ground samples with KBr granules were recorded on a Tensor 27IR Fourier-transform spectrometer (Bruker, Germany) in the 4000—400 cm^{-1} frequency range with a spectral resolution of 4 cm^{-1}.

The sedimentation kinetics in aqueous suspensions of MCM-41 was studied using a Specord 250 Plus spectrophotometer (Analytik Jena), registering the optical density at a fixed wavelength (λ = 320 nm) for 10 min.

Results and Discussion

Characterization of the sample by scanning electron microscopy (SEM). Microphotographs obtained by SEM show that the synthesized MCM-41 is formed by particles with a diameter of 100—200 nm with a highly developed surface (Fig. 1).

Dimensional and charge characteristics of dispersions of mesoporous silica in water. Dynamic and electrophoretic light scattering were used to assess the dimensional and charge characteristics of dispersions of pure MCM-41. The concentration of the dispersed phase in the colloidal system was selected empirically and was equal to 0.01 mg mL^{-1}. A bimodal size distribution of aggregates was observed for the given mesoporous silica content in the system (Fig. 2). The majority of the formed aggregates were particles with a hydrodynamic diameter $D_h \approx 175$ nm, with an insignificant (~5%) contribution of larger particles with $D_h \approx 600$ nm. The obtained results for the most part satisfy the requirements imposed on drug carriers ($D_h \leq 200$ nm) adopted for prolonged circulation in the circulatory system.

Electrophoretic light scattering demonstrated that MCM-41 particles in an aqueous solution are negatively charged (–40 mV, Fig. 3). This result indicates a high stability of systems based on MCM-41 upon their dispersion due to the electrostatic repulsive forces preventing particle agglomeration.

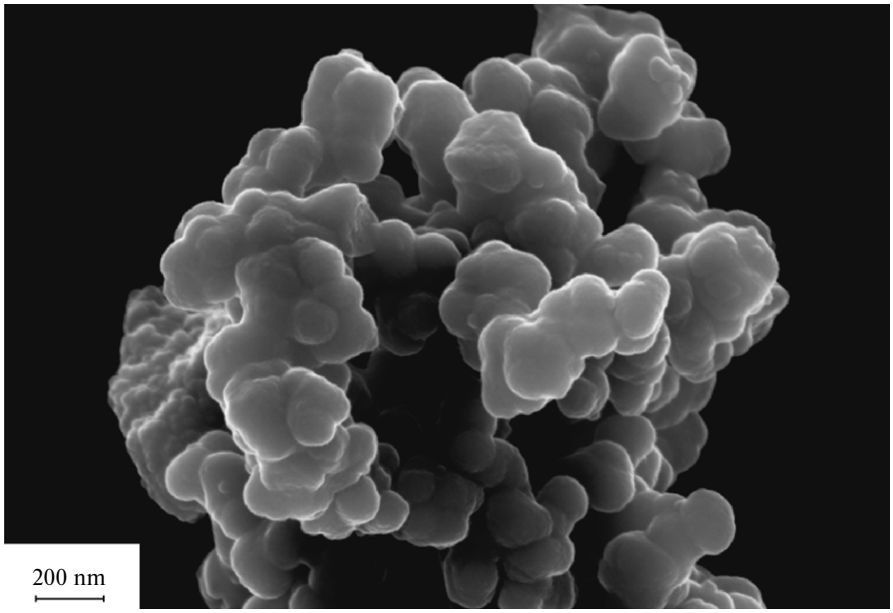

Fig. 1. Micrograph of MCM-41 particles obtained using a scanning electron microscope.

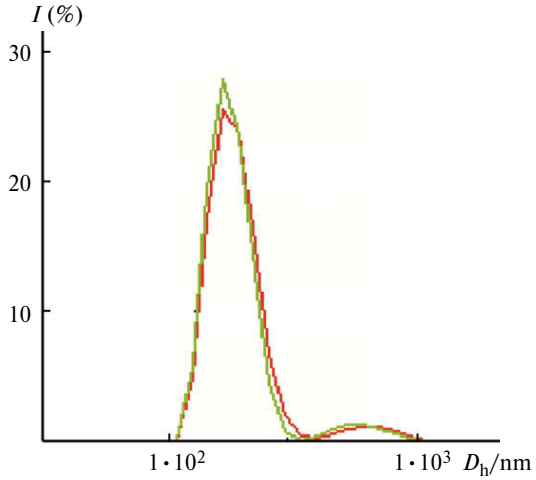

Fig. 2. Particle-size distribution for the suspension of mesoporous silica in water averaged by the number of particles; $C = 0.01$ mg mL^{-1}; 25 °C.
Note. Figures 2, 3 and 8 are available in full color on the web page of the journal (https://link.springer.com/journal}/volumesAndIssues/11172).

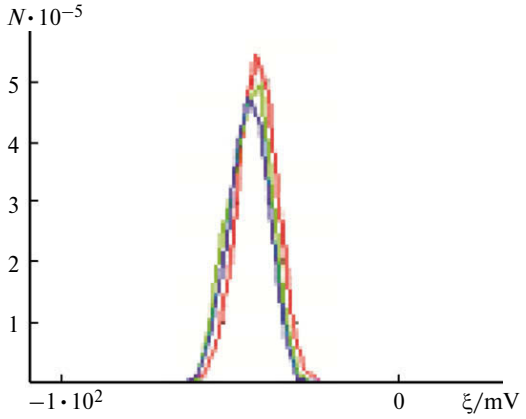

Fig. 3. Electrophoretic light scattering results characterizing the electrokinetic potential of particles in the mesoporous silica suspension in water; $C = 0.01$ mg mL^{-1}; 25 °C; N is the number of counts.

Characterization of the sample by X-ray diffraction. X-ray diffraction results (Table 1) confirm the presence of an ordered hexagonal structure of the obtained mesoporous silica sample. The presence of four reflections from the planes (100), (110), (200), and (210) on the diffraction pattern indicates a fairly high degree of hexagonal architecture in the sample. The interplanar spacing, calculated from the positions of peak maxima, corresponds to a mean hexagonal lattice parameter a equal to 39.4 Å. According to literature, the lattice parameter a of MCM-41 type mesoporous silica is in the range 40—54 Å.[21,29,37,38]

Sedimentation parameters of aqueous suspensions of MCM-41. To assess the prospects for the use of suspensions based on MCM-41 with an adsorbed drug in biotechnology, it is important to examine the rates of sedimentation of MCM-41 suspensions in water. In the first stage of study, electronic spectra of sedimentating MCM-41 over time were recorded (Fig. 4). As can be seen, silica particles sediment with time, which leads to a clearing of the solution, *i.e.*, to a decrease of absorption intensity. The change in the optical density was the most noticeable in the range of 200—400 nm, therefore, the sedimentation kinetics was further studied at a wavelength of 300 nm, recording the dependence of optical density at the given wavelength over time. The dependence obtained over 5 min in the kinetic experiment is shown in Fig. 4 (see inset). Approximately 18% of the MCM-41 coarse suspension sank over 5 min. At high contents of silica particles in aqueous dispersions, most of the powdered MCM-41 sank at a high rate, which is beyond measurements. Due to this, these measurements can be made with a considerably lower accuracy. Therefore, further studies were carried out for systems with a low MCM-41 content. For this purpose, the sedimentation kinetics of mesoporous silica with a MCM-41 content of 0.06, 0.18, and 0.3 wt.% were studied. The obtained results are shown in Fig. 5, which indicate that at a minimum content of MCM-41 (0.06 wt.%), the changes in optical density over 10 min are minor and the system is almost completely stable and sedimentation is minimal. An increase in the content of mesoporous silica to 0.18 and 0.3 wt.% considerably increases sedimentation processes in the system, which is

Table 1. X-ray characteristics for MCM-41 type mesoporous silica particles

Reflection indices (*hkl*)	Interplanar spacing (d/Å)	2θ/deg
100	33.985	2.598
110	19.834	4.452
200	17.136	5.153
210	13.022	6.783

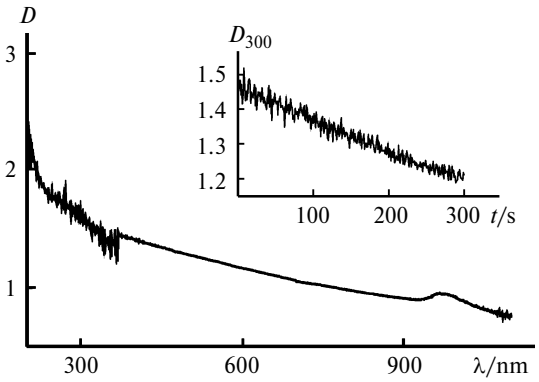

Fig. 4. Electronic absorption spectrum of MCM-41 sedimentation in water; 25 °C.

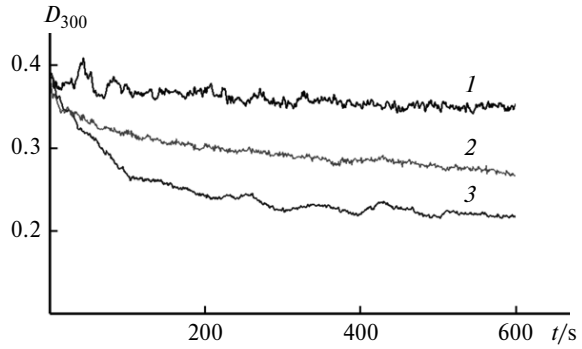

Fig. 5. Kinetic sedimentation curves of aqueous dispersions of MCM-41 with the dispersed phase content of 0.06 (*1*), 0.18 (*2*), and 0.3 wt.% (*3*); 25 °C.

reflected in a substantial change in optical density compared to the initial value. In this case, it can be deduced that 30—45% of the starting amount of silica is involved in sedimentation.

Spectrophotometric analysis of indomethacin encapsulation. The content of encapsulated indomethacin in the mesopores of MCM-41 silica was determined using spectrophotometry. Figure 6 shows the results characterizing the amount of indomethacin contained in ethanol washings after the encapsulation of the drug into the carrier pores over 3 h at a temperature of 40 and 60 °C.

The presence of the drug in ethanol washings can result either from a low degree of loading of indomethacin into the pores of MCM-41 or from the removal of the adsorbate from the primary adsorption sites located on the outer surface and the inner walls of silica pores. The dominant of these two factors can be determined from the results of calculations based on spectrophotometric measurements

Table 2. Quantitative characteristics of indomethacin encapsulation into MCM-41 mesoporous silica particles during the interaction of components at temperatures 40 °C (MCM-41@IMC-40) and 60 °C (MCM-41@IMC-60) obtained by various methods

Sample	TG analysis, m/mg g^{-1}	Spectrophotometry	
		E_{inc}	E_{load}
		%	
MCM-41@IMC-40	28.6	53.0	17.7
MCM-41@IMC-60	41.8	99.6	22.3

(Table 2). It was shown that in both cases studied, a practically quantitative encapsulation of indomethacin into the pores of the silica carrier was achieved with a high (over 30%) drug loading efficiency. Thus, it can be argued that the presence of a small amount of unbound indomethacin is a result of the drug removal from the pores of MCM-41.

Study of adsorption—desorption of N_2. The isotherms of nitrogen adsorption—desorption and the size distribution of MCM-41 particle pores before and after the encapsulation of indomethacin are shown in Fig. 7. The obtained adsorption pattern for silica particles in the absence of a drug substance is a type IV isotherm characteristic for mesoporous adsorbents.[11] It was shown that in both cases, the isotherms showed a sharp increase at a relative pressure of $0.2 \le p/p_0 \le 0.4$, which is related to capillary condensation of nitrogen in the channels and to a narrow size distribution of pores (Fig. 8). The analysis of textural parameters of the MCM-41 and MCM-41@IMC-40 samples determined by this method showed that the transition from the first system to the second is ac-

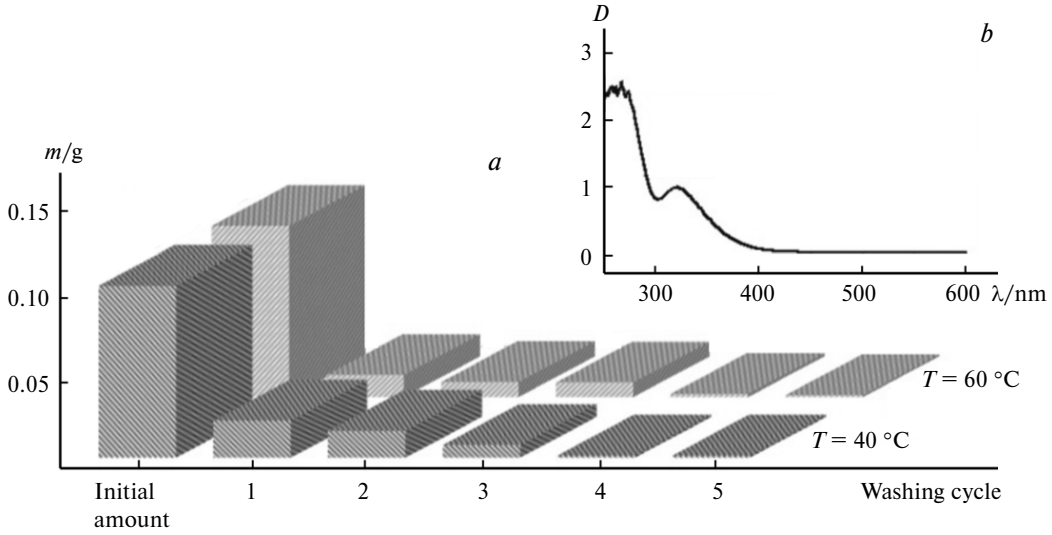

Fig. 6. Change in the content of indomethacin (m) in washing ethanol with varying temperature and number of washing cycles determined by spectrophotometry (*a*) and electronic absorption spectrum of washing ethanol containing non-encapsulated indomethacin (*b*).

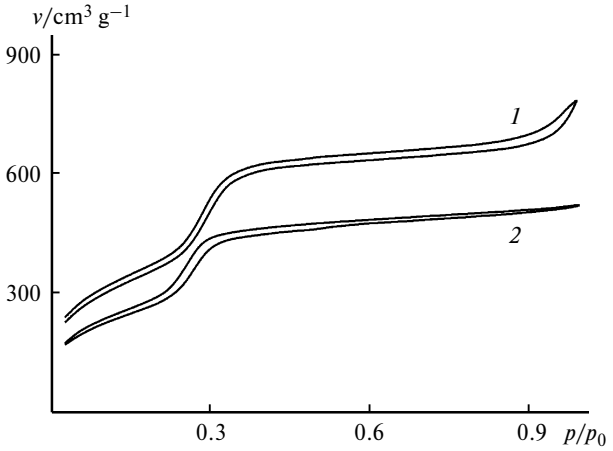

Fig. 7. Nitrogen adsorption—desorption isotherms for MCM-41 mesoporous silica particles in the absence (*1*) and in the presence (*2*) of encapsulated indomethacin.

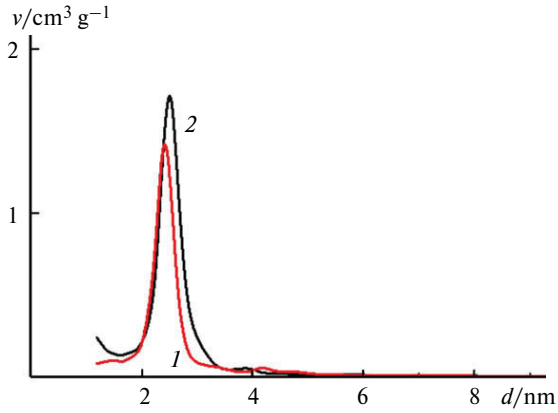

Fig. 8. Pore-size distribution for MCM 41 mesoporous silica particles in the presence (*1*) and in the absence of indomethacin (*2*), calculated using the BJH model.

companied by a decrease in the volume of adsorbed nitrogen (see Fig. 7), which indicates a partial filling of the pores. Therefore, the corresponding values of specific surface area and volume of pores of the mesoporous silica sample decrease after the contact with indomethacin (Table 3).

IR spectra. To characterize the encapsulated indomethacin in the mesopores of MCM-41 silica, IR spectra were recorded for MCM-41@IMC system and its components in the individual state (Fig. 9). Spectrum *1*, corresponding to individual MCM-41, is typical of mesoporous materials and contains their characteristic bands. For example, the bands at 966 and 462 cm^{-1} correspond to stretching vibrations of the Si—O bonds and bending vibrations of the Si—O fragment of the surface Si—O—H groups, respectively. In addition, antisymmetric stretching vibrations of the Si—O—Si bonds at 1237 cm^{-1} located on the surface of particles and within them can be clearly distinguished (1084 cm^{-1} (ν_{as} SiO_4) and 797 cm^{-1} (ν_{sym} SiO_4))

Table 3. Physicochemical characteristics of MCM-41 mesoporous silica particles before and after contact with indomethacin

System	Pore volume* /cm^3 g^{-1}	Pore diameter* /nm	Specific surface area /m^2 g^{-1}
MCM-41	1.336	2.5	1927.1
MCM-41@IMC	0.902	2.3	976.7

* Calculated using the BJH method.

(see Fig. 9). The bands at about 3454 and 1636 cm^{-1} are related to stretching and bending vibrations of physiosorbed water, respectively. There is a characteristic narrow band at 3745 cm^{-1} corresponding to vibrations of the OH groups in isolated silanol groups and a weak band at 3650 cm^{-1} attributed to vibrations of terminal silanol groups. The absence of a band at 3745 cm^{-1} is probably due to a smaller number of defects in the silicon-oxygen skeleton in the walls of large pores and, accordingly, a smaller number of silanol group.

IR spectra of indomethacin in the individual state (see Fig. 9, spectrum *2*) are characterized by the band maxima related to stretching vibrations of the carbonyl fragment of the carboxyl group (at 1714 cm^{-1}), belonging to the amide group (at 1692 cm^{-1}), and characteristic vibrations of carbon atoms of aromatic fragments (at 1479 cm^{-1}).

After contact with indomethacin (see Fig. 9, spectra *3* and *4*), the bands at 1706 and 1463 cm^{-1} appear in the spectra of mesoporous silica samples, corresponding to stretching vibrations of the carboxy C=O group and phenyl fragments, respectively, which confirm that the drug was successfully encapsulated into the mesoporous material. In contrast to indomethacin in the free state, this system demonstrates a considerable weakening of these bands and their shift toward lower wavenumbers. This is probably due to the fact that carboxyl and heterocyclic fragments

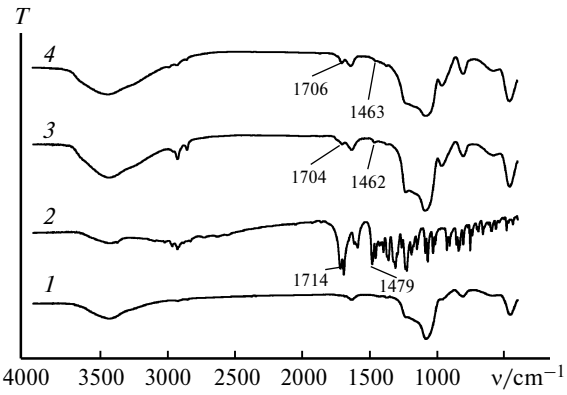

Fig. 9. IR spectra of MCM-41 type mesoporous silica in the free state (*1*), individual indomethacin (*2*) and MCM-41 particles after contact with indomethacin at a temperature of 40 (*3*) and 60 °C (*4*).

in indomethacin molecules form hydrogen bonds with silanol groups localized on the silicon dioxide surface. The variation of IR band intensities from samples obtained upon contact with the drug at different temperatures can be explained by varying percentage of drug encapsulated in the pores. Thus, the amount of drug bound to the carrier can be regulated by varying the temperature of encapsulation of the drug into mesoporous silica particles.

TG analysis. To determine the amount of indomethacin encapsulated in the pores of silica particles, TG analysis of MCM-41 in the free state and MCM-41 loaded with indomethacin was carried out at temperatures 40 and 60 °C (Fig. 10). The obtained TG curves indicate the different character of weight loss that occurs when MCM-41, MCM-41@IMC-40, and MCM-41@IMC-60 samples are heated: the weight of the samples decreases from 95.6 to 85.5%. The initial loss of weight in all the samples in the temperature range from 25 to 110 °C corresponds to the desorption of water molecules from the mesoporous matrix. The matrix of pure MCM-41 silica in the studied temperature range from 110 to 1000 °C is thermostable (see Fig. 10, curve *1*) and the loss of weight (1.5%) occurs in one step at 65.3 °C. The presence of encapsulated indomethacin molecules in mesoporous silica particles led to the appearance of endothermic peaks at 145.7 and 496.6 °C for MCM-41@IMC-40 and MCM-41@IMC-60 (Fig. 11). The total weight loss over the temperature range 200—700 °C, corresponding to the decomposition of indomethacin, was 2.86 and 4.18% for MCM-41@IMC-40 and MCM-41@IMC-60, respectively (see Fig. 10, curves *2* and *3*). This indicates that when indomethacin contacts with mesoporous silica at temperatures 40 and 60 °C, 28.6 mg and 41.8 mg of the drug are encapsulated in 1 g of MCM-41, respectively (see Table 1). This value is considerably higher than the maximum amount of drug encapsulated into MCM-41 particles found earlier.[25]

In conclusion, a MCM-41 type mesoporous material was synthesized that is superior to the known analogs in terms of specific surface and volume of pores. An efficient protocol for the encapsulation of a hydrophobic drug was developed using indomethacin as a test material. The

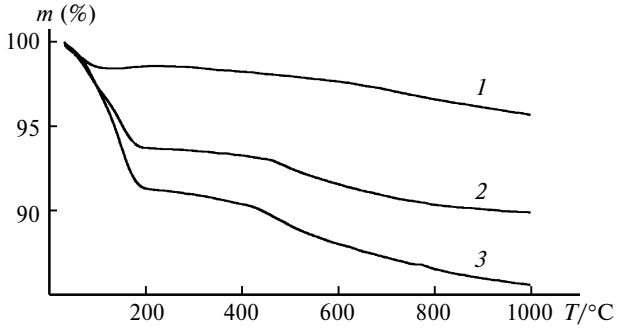

Fig. 10. Thermogravimetric curves of samples of MCM-41 (*1*), MCM-41@IMC-40 (*2*), and MCM-41@IMC-60 (*3*).

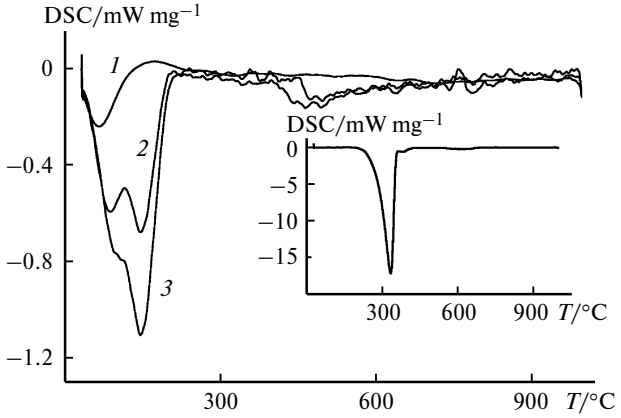

Fig. 11. DSC thermograms for MCM-41 (*1*), MCM-41@IMC-40 (*2*), and MCM-41@IMC-60 samples (*3*); in the inset, a DSC thermogram for individual indomethacin.

obtained results allow us to recommend the mesoporous material described above as a promising carrier for a wide range of lipophilic drugs.

The work was performed using the instrumental park of the Spectral-Analytical Center of Shared Facilities for Study of Structure, Composition and Properties of Substances and Materials of the Arbuzov Institute of Organic and Physical Chemistry, a separate structural unit of the Federal Recearch Center "Kazan Scientific Center of the Russian Academy of Sciences".

This work was financially supported by the Russian Foundation for Basic Research (Project No. 18-03-00591).

References

1. D. A. Kharkevich, *Farmakologiya* [*Pharmacology*], GEOTAR-Media, Moscow, 2013, 760 pp. (in Russian).
2. *Klinicheskaya farmakologiya* [*Clinical Pharmacology*], Ed. V. G. Kukes, GEOTAR-Media, Moscow, 2006, 938 pp. (in Russian).
3. A. P. Kaplun, D. A. Bezrukov, V. I. Shvets, *Biotekhnologiya* [*Biotechnology*], 2010, No. 6, 9 (in Russian).
4. V. S. Ulashchik, *Voprosy kurortologii, fizioterapii i lechebnoi fizicheskoi kul'tury* [*Problems of Balneology, Physiotherapy, and Therapeutic Physical Culture*], 2014, No. 6, 52 (in Russian).
5. B. Tzankov, K. Yoncheva, M. Popova, A. Szegedi, G. Momekov, J. Mihaly, N. Lambov, *Micropor. Mesopor. Mater.*, 2013, **171**, 131.
6. I. I. Slowing, J. L. Vivero-Escoto, C.-W. Wu, S.-Y. Lin, *Adv. Drug Deliv. Rev.*, 2008, **60**, 1278.
7. B. C. Hancock, *J. Pharm. Pharmacol.*, 2002, **54**, 737.
8. E. T. Cole, D. Cadé, H. Benameur, *Adv. Drug Deliv. Rev.*, 2008, **60**, 747.
9. C. Leuner, J. Dressman, *Eur. J. Pharm. Biopharm.*, 2000, **50**, 47.
10. T. Vasconcelos, B. Sarmento, P. Costa, *Drug Discov. Today*, 2007, **12**, 1068.
11. K. S. W. Sing, D. H. Everett, R. A. W. Haul, L. Moscou, R. A. Pierotti, J. Rouquerol, T. Siemieniewska, *Pure Appl. Chem.*, 1985, **57**, 603.

12. S. P. Hudson, R. F. Padera, R. Langer, D. S. Kohane, *Biomaterials*, 2008, **29**, 4045.
13. J. Shi, X. Sun, Sh. Zheng, J. Li, X. Fu, H. Zhang, *Biomaterials*, 2018, **152**, 15.
14. J. Yang, L. Fan, F. Wang, Y. Luo, X. Sui, W. Li, X. Zhang, Y. Wang, *Nanoscale*, 2016, **8**, 9537.
15. J. Shi, Y. Hedberg, M. Lundin, I. Odnevall Wallinder, H. L. Karlsson, L. Möller, *Acta Biomater.*, 2012, **8**, 3478.
16. Z. Gounani, M. A. Asadollahi, R. L. Meyer, A. Arpanaei, *Int. J. Pharm.*, 2018, **537**, 148.
17. S. Seré, B.De Roo, M. Vervaele, S. Van Gool, S. Jacobs, J. W. Seo, J.-P. Locquet, *J. Nanomater., 2*018, **2018**, 7390618.
18. J. G. Croissant, Y. Fatieiev, N. M. Khashab, *Adv. Mater.*, 2017, **29**, 1604634.
19. J. Weitkamp, *Solid State Ionics*, 2000, **131**, 175.
20. Y. Wan, D. Zhao, *Chem. Rev.*, 2007, **107**, 2821.
21. Z. Liu, Y. Wei, Y. Qi, S. Zhang, Y. Zhang, Z. Liu, *Micropor. Mesopor. Mater.*, 2006, **93**, 205.
22. L. Latifi, Sh. Sohrabnezhad, M. Hadavi, *Micropor. Mesopor. Mater.*, 2017, **250**, 148.
23. G. Kaptay, *Int. J. Pharm.*, 2012, **430**, 253.
24. T. Cordeiro, C. Castiñeira, D. Mendes, F. Danède, J. Sotomayor, I. M. Fonseca, M. Gomes da Silva, A. Paiva, S. Barreiros, M. M. Cardoso, M. T. Viciosa, N. T. Correia, M. Dionisio, *Mol. Pharm.*, 2017, **14**, 3164.
25. A. Gignone, L. Manna, S. Ronchetti, M. Banchero, B. Onida, *Micropor. Mesopor. Mater.*, 2014, **200**, 291.
26. Y. Wang, Q. Zhao, Y. Hu, L. Sun, L. Bai, T. Jiang, S. Wang, *Int. J. Nanomed.*, 2013, **8**, 4015.
27. T. Ukmar, U. Maver, O. Planinsek, A. Pintar, V. Kauci, A. Godec, M. Gaberscek, *J. Mater. Chem.*, 2012, **22**, 1112.
28. A. Mathew, S. Parambadath, S. S. Park, Ch.-S. Ha, *Micropor. Mesopor. Mater.*, 2014, **200**, 124.
29. W. R. Braz, N. L. Rocha, H. de Faria Emerson, M. L. A. Silva, K. J. Ciuffi, D. C. Tavares, R. A. Furtado, L. A. Rocha, E. J. Nassar, *Nanotechnology*, 2016, **27**, 385103.
30. L. Hu, Ch. Sun, A. Song, D. Chang, X. Zheng, Y. Gao, T. Jiang, S. Wang, *Asian J. Pharm. Sci.*, 2014, **9**, 183.
31. C. J. Shorrock, W. D. Rees, *Gut*, 1992, **33**, 164.
32. H. Long, W. Wang, W. Yang, Y. Wang, H. Ru, *Micropor. Mesopor. Mater.*, 2018, **263**, 34.
33. Q. Cai, W.-Y. Lin, F.-Sh. Xiao, W.-Q. Pang, X.-H. Chen, B.-S. Zou, *Micropor. Mesopor. Mater.*, 1999, **32**, 1.
34. L. Zakharova, Yu. Kudryashova, A. Ibragimova, E. Vasilieva, F. Valeeva, E. Popova, S. Solovieva, I. Antipin, Yu. Ganeeva, T. Yusupova, A. Konovalov, *Chem. Eng. J.*, 2012, **185—186**, 285.
35. S. J. Gregg, K. S. W. Sing, *Adsorption, Surface Area, and Porosity*, Academic Press, 1982, 304 pp.
36. E. P. Barrett, L. G. Joyner, P. P. Halenda, *J. Am. Chem. Soc.*, 1951, **73**, 373.
37. C. T. Kresge, M. E. Leonowicz, W. J. Roth, J. C. Vartuli, J. S. Beck, *Nature*, 1992, **359** 6397.
38. U. Ciesla, F. Schüth, *Micropor. Mesopor. Mater.*, 1999, **27**, 131.

Received November 29, 2018;
in revised form February 20, 2019;
accepted March 7, 2019